QALAAI ZANISTSCIENTIFIC JOURNAL
A Scientific Quarterly Refereed Journal Issued by Lebanese French University – Erbil, Kurdistan, Iraq
Vol. (10), No (1), Spring 2025
ISSN 2518-6566 (Online) - ISSN 2518-6558 (Print)

Residual Stress Analysis for Composite Thermoplastic Woven Material with Unique Bending Moment: Analytical and Finite Element Analysis

Azad Mohammed Ali Saber
Department of Aviation, College of Engineering, Salahaddin University, Erbil Kurdistan Region, Iraq.
Email: Azad.saber@su.edu.krd

Lanja Saeed Omer
Department of Mechanical and Mechatronics, College of Engineering, Salahaddin University, Erbil Kurdistan Region, Iraq.
Email: Lanja.omer@su.edu.krd

ARTICLE INFO

Article History:
Received: 23/8/2023
Accepted: 12/12/2023
Published: Spring 2025

Keywords:
Residual stresses, Thermoplastic composite, Elastic-plastic solution, Finite Element, APDL Ansys

Doi:
10.25212/lfu.qzj.10.1.42

ABSTRACT

Analytical analysis for assumption of the Bernoulli-Navier hypotheses and finite element method (APDL) are used to detect the residual stress through composite beam under unique bending moment for various elastic-plastic boundaries. A woven steel fibers with various orientation angles (0^o, 15^o, 30^o, 45^o, 60^o, and 90^o) is assumed in this analysis. The governing differential equation and the boundary conditions are both resolved analytically for plane stress case and tiny plastic deformations. The yield criterion is based on the Tsai-Hill theory. It is observed that; the residual stress intensity is strongest at the top and bottom roofs of the beam. A good agreement is found between analytical and finite element method for several moments M and elastic-plastic boundary h.

QALAAI ZANISTSCIENTIFIC JOURNAL
A Scientific Quarterly Refereed Journal Issued by Lebanese French University – Erbil, Kurdistan, Iraq
Vol. (10), No (1), Spring 2025
ISSN 2518-6566 (Online) - ISSN 2518-6558 (Print)

Nomenclature

(a, b)	Equation Coefficients
(A, B)	Lower and Center Beam Positions
$2C$	Beam Height
(h_1, h_2, h)	Elastic-Plastic Boundary
I	Moment of Inertia
L	Beam Length
M	Bending Moment
w	Beam Thickness
(x, y)	Cartesian Dimensions
(X, Y, Z)	Principal Yield Materials in Three Axis
Δ	Stress Function
$\bar{\lambda}_{ij}$	Compliance Matrix Components
$(\varepsilon_x, \varepsilon_y, \gamma_{xy})$	Strain Components
$(\varepsilon_1, \varepsilon_2, \tau_{12})$	Principal Strain Components
σ_x	Stress Component
σ_y	Yield Stress
σ_{eq}	Equivalent Principal Stress
$(\sigma_1, \sigma_2, \tau_{12})$	Principal Stress Components
$(\Gamma_1, \Gamma_2, \Gamma_3, \Gamma_4, \Gamma_5, \Gamma_6, \Gamma_7)$	Integration Constants
$(\mathrm{K}_1, \mathrm{K}_2, \mathrm{K}_3)$	Plastic Strain Coefficients

1. Introduction

The publicity of thermoplastic composites is rising as a result of their many utilities. They provide enhanced fracture toughness, high specific stiffness, specific strength, and higher resistance to impact. further to this, thermoplastic composites can be created without drawn-out curing procedures and do not demand complicated chemical reactions to be processed. They are reprocessing able, reconfigurable, and remelt able. [1–4] include experimental researches on the formation of thermoplastic composites.

In composites, residual stresses are especially significant because they have the potential to either strengthen the material or induce precocious failure. Using the finite element method, [5] performed an elasto-plastic stress analyses of anisotropic

QALAAI ZANISTSCIENTIFIC JOURNAL
A Scientific Quarterly Refereed Journal Issued by Lebanese French University – Erbil, Kurdistan, Iraq
Vol. (10), No (1), Spring 2025
ISSN 2518-6566 (Online) - ISSN 2518-6558 (Print)

plates and shells. As a yield criterion, they employed the Huber-Mises plastic theory. In carbon-fiber thermoplastic matrix laminates, residual stresses were detected by [6]. For carbon fiber/thermoplastic composites, a user material subroutine in ABAQUS was used to create a computational finite element (FE) model of thermal residual stress [7]. The temperature gradient on the simulated stresses as well as the axial and transverse orientations of the fiber with the stresses within a typical volume element at the top and bottom surfaces of the composite layer were investigated [8] . [9] studied the effects of residual stress on the mechanical and thermal characteristics of injection-molded thermoplastics. Using an analytical solution, [10] performed an elastoplastic stress analysis on a cantilever beam made of aluminum metal matrix composites that was loaded by a single force at the free end and a uniformly distributed force at the upper surface. Using the finite element method (FEM), the elastic-plastic stress analysis of anisotropic plates, shells and orthotropic rotating discs with holes are performed [11–15]. In a metal matrix composite cantilever beam, an analytical research of elastic-plastic stress analysis is conducted [16].

The analytical models for measuring the macro residual stresses or ply scale in polymeric composite materials are covered in [17]. A good agreement is found between stresses measured using a constant stress approximation approach provided the best agreement with measurements obtained using the layer removal technique [18]. The residual stress and deformation in specimens made of short carbon fiber reinforced, carbon nanotube reinforced, and unreinforced acrylonitrile-butadiene-styrene are described in [19]. [20] investigated process-induced stresses brought on by the interaction of mold and composites, taking into account the behavior of composite materials in relation to temperature and time, and it is suggested a new numerical step-by-step scheme to take into account mechanisms of stress generation and stress release. With particular focus on the macroscopic stresses that arise on a ply-to-ply level, residual stresses that are formed in continuous carbon-fiber-reinforced thermoplastic composites are examined [21]. To detect the influence of ply orientation on the evolution of residual stress, five symmetric and asymmetric layup configurations are examined [22]. To describe the deformation after the thermal cycle, a number of computer-aided engineering (CAE) analyses were carried

QALAAI ZANISTSCIENTIFIC JOURNAL
A Scientific Quarterly Refereed Journal Issued by Lebanese French University – Erbil, Kurdistan, Iraq
Vol. (10), No (1), Spring 2025
ISSN 2518-6566 (Online) - ISSN 2518-6558 (Print)

out, including injection-molding analysis and finite element analysis (FEA) [23]. [24] reviewed the experimental methods for estimating residual stress in thermosetting fiber reinforced composites. In the current work an elastic/plastic stress analysis is performed in a woven steel fiber reinforced low density thermoplastic composite cantilever beam loaded by a bending moment at its free end. Small plastic deformations are assumed in Tsai-Hill theory approach. The beam is taken into account during the problem's solution as linearly hardening. Bernoulli-Navier hypothesis is utilized in this work. The thermoplastic composite steel fiber reinforcement beam was chosen to achieve some plastic deformations in order to confirm the analytical theory. APDL ANSYS software version 19 is used to model composite laminated structure using finite element method.

2. Elastic Analysis

2.1 Governing Relations

The governing differential equations for composite beam structure shown in Fig.1 are solved using plane stress state as illustrated in [17]

$$\bar{\lambda}_{22}\frac{\partial^4\Delta}{\partial x^4} - 2\bar{\lambda}_{26}\frac{\partial^4\Delta}{\partial x^3\partial y} + \left(2\bar{\lambda}_{12} + \bar{\lambda}_{66}\right)\frac{\partial^4\Delta}{\partial x^2\partial y^2} - 2\bar{\lambda}_{16}\frac{\partial^4\Delta}{\partial x\partial y^3} + \bar{\lambda}_{11}\frac{\partial^4\Delta}{\partial y^4} = 0 \qquad (1)$$

The stress-strain relation is given in [18] as

$$\begin{Bmatrix}\varepsilon_x\\ \varepsilon_y\\ \gamma_{xy}\end{Bmatrix} = \begin{bmatrix}\bar{\lambda}_{11} & \bar{\lambda}_{12} & \bar{\lambda}_{16}\\ \bar{\lambda}_{12} & \bar{\lambda}_{22} & \bar{\lambda}_{26}\\ \frac{\bar{\lambda}_{16}}{2} & \frac{\bar{\lambda}_{26}}{2} & \frac{\bar{\lambda}_{66}}{2}\end{bmatrix}\begin{Bmatrix}\sigma_x\\ \sigma_y\\ \tau_{xy}\end{Bmatrix} \qquad \bar{\lambda}_{ij} = f\left(\lambda_{ij},\theta\right)\ \&\ \lambda_{ij} = f\left(E_{ij},G_{ij},\nu_{ij}\right) \qquad (2)$$

Figure 1 depicts a composite cantilever beam geometry undergo under a moment at the free end.

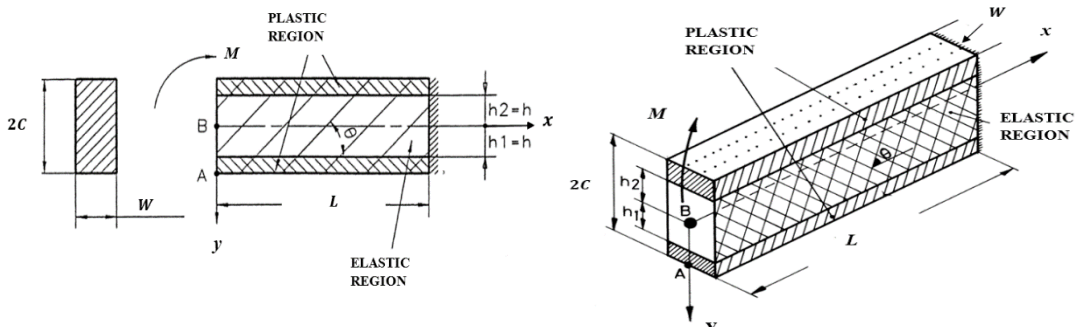

QALAAI ZANISTSCIENTIFIC JOURNAL
A Scientific Quarterly Refereed Journal Issued by Lebanese French University – Erbil, Kurdistan, Iraq
Vol. (10), No (1), Spring 2025
ISSN 2518-6566 (Online) - ISSN 2518-6558 (Print)

Figure (1): Composite Cantilever Beam Geometry ($L = 100mm, W = 7mm, C = 6mm$)

2.2 Boundary Condition Relations

The governing equations and boundary conditions are solved simultaneously using the relation $\Delta = \frac{R}{6}y^3$ where $R = M/I$ and $I = 2wc^3/3$

At the free end $M = \int_{-C}^{C} \sigma_x y w dy$ (3)

$\sigma_y = 0 \ , \ \tau_{xy} = 0$ at $y = \pm c$ (4)

$\sigma_x = \frac{\partial^2 \Delta}{\partial y^2} = Ry \ , \quad \sigma_y = \frac{\partial^2 \Delta}{\partial x^2} = 0 \ , \quad \& \quad \tau_{xy} = -\frac{\partial^2 \Delta}{\partial x \partial y} = 0$ (5)

2.3 Deformations Relations

Using strain/displacement equations, the displacement relations can be obtained by relations as

$$\varepsilon_x = \frac{\partial u}{\partial x} = \bar{\lambda}_{11}\sigma_x = R\bar{\lambda}_{11}y \qquad \varepsilon_y = \frac{\partial v}{\partial y} = \bar{\lambda}_{12}\sigma_x = R\bar{\lambda}_{12}y$$

$$\varepsilon_{xy} = \frac{1}{2}\left(\frac{\partial u}{\partial y} + \frac{\partial v}{\partial x}\right) = \frac{\bar{\lambda}_{16}}{2}\sigma_x = R\frac{\bar{\lambda}_{16}}{2}y \quad (6)$$

Using the integration of equations (6) results the displacement relations as

$u = R\bar{\lambda}_{11}xy + \Gamma_1(y) \ , \quad \& \quad v = R\frac{\bar{\lambda}_{12}}{2}y^2 + \Gamma_2(x)$ (7)

$u = v = \frac{\partial v}{\partial x} = 0$ at $(x = L, y = 0)$ (B.C's at the fixed end) (8)

After substituting eq. (7) into ε_{xy} and applying the boundary conditions, it results the displacement relations in the elastic region as follows

$u = R\bar{\lambda}_{11}xy + \frac{R\bar{\lambda}_{16}y^2}{2} - R\bar{\lambda}_{11}Ly \ \& \ v = \frac{R\bar{\lambda}_{12}y^2}{2} - \frac{R\bar{\lambda}_{11}x^2}{2} + R\bar{\lambda}_{11}Lx - \frac{R\bar{\lambda}_{11}L^2}{2}$ (9)

QALAAI ZANISTSCIENTIFIC JOURNAL
A Scientific Quarterly Refereed Journal Issued by Lebanese French University – Erbil, Kurdistan, Iraq
Vol. (10), No (1), Spring 2025
ISSN 2518-6566 (Online) - ISSN 2518-6558 (Print)

3. Elastic-Plastic Analysis

3.1 Governing Relations

Due to the similarity of yield zones in principal material directions ($X = Y = Z$), Tsai-Hill theory is utilized in this analysis. The yield criteria are given by [18] as

$$\frac{\sigma_1^2}{X^2} + \frac{\sigma_2^2}{Y^2} - \left(\frac{1}{X^2} + \frac{1}{Y^2} - \frac{1}{Z^2}\right)\sigma_1\sigma_2 + \frac{\tau_{12}^2}{S^2} = 1 \tag{10}$$

The first principal stress is derived as

$$\sigma_{eq} = \bar{\sigma} = \sqrt{\sigma_1^2 - q\sigma_1\sigma_2 + \frac{X^2\sigma_2^2}{Y^2} + \frac{X^2\tau_{12}^2}{S^2}}\ , \quad q = \left(1 + \frac{X^2}{Y^2} - \frac{X^2}{Z^2}\right) \tag{11}$$

Where $\sigma_1 = \sigma_x cos^2\theta,\ \sigma_2 = \sigma_x sin^2\theta, \& \tau_{12} = -\sigma_x cos\theta sin\theta$ (12)

For plastic zone, the equilibrium's equations are given as

$$\frac{\partial\sigma_x}{\partial x} + \frac{\partial\tau_{xy}}{\partial y} = 0 \quad \& \quad \frac{\partial\tau_{xy}}{\partial x} + \frac{\partial\sigma_y}{\partial y} = 0 \tag{13}$$

Using Ludwik equation, the plastic stress equation is written as

$$\sigma_y = X + K\varepsilon_p \tag{14}$$

Putting the stress components ($\sigma_1, \sigma_2, \& \tau_{12}$) into σ_{eq} results the yield stress state as function of θ

$$X_1 = \frac{X}{P}\ ,\ P = \sqrt{cos^4\theta - qsin^2\theta cos^2\theta + \frac{X^2 sin^4\theta}{Y^2} + \frac{X^2 sin^2\theta cos^2\theta}{S^2}}, \quad \sigma_x = \frac{\sigma_y}{P} \tag{15}$$

The plastic strain additions in the principal material directions are detected using the potential function g [19]

$$\begin{Bmatrix} d\varepsilon_1^p \\ d\varepsilon_2^p \\ d\gamma_{12}^p \end{Bmatrix} = \begin{Bmatrix} \frac{\partial g}{\partial\sigma_1} d\Gamma \\ \frac{\partial g}{\partial\sigma_2} d\Gamma \\ \frac{\partial g}{\partial\tau_{12}} d\Gamma \end{Bmatrix} \tag{16}$$

QALAAI ZANISTSCIENTIFIC JOURNAL
A Scientific Quarterly Refereed Journal Issued by Lebanese French University – Erbil, Kurdistan, Iraq
Vol. (10), No (1), Spring 2025
ISSN 2518-6566 (Online) - ISSN 2518-6558 (Print)

The total strain increments in the principal material directions are given as

$$d\varepsilon_1 = d\varepsilon_1^e + d\varepsilon_1^p = \lambda_{11}d\sigma_1 + \lambda_{12}d\sigma_2 + \frac{2\sigma_1 - q\sigma_2}{2\sigma_y}d\Gamma$$

$$d\varepsilon_2 = d\varepsilon_2^e + d\varepsilon_2^p = \lambda_{12}d\sigma_1 + \lambda_{22}d\sigma_2 + \frac{-q\sigma_1 + \frac{2\sigma_2 X^2}{Y^2}}{2\sigma_y}d\Gamma$$

$$d\gamma_{12} = d\gamma_{12}^e + d\gamma_{12}^p = \frac{\lambda_{66}d\tau_{12}}{2} + \frac{\frac{2\tau_{12}X^2}{S^2}}{2\sigma_y}d\Gamma \quad (17)$$

Substituting $\sigma_1, \sigma_2, \& \tau_{12}$ into eq. (17) with integrating them results:

$$\varepsilon_1 = \lambda_{11}\sigma_1 + \lambda_{12}\sigma_2 + \frac{2cos^2\theta - qsin^2\theta}{2P}\varepsilon_p + \Gamma_3$$

$$\varepsilon_2 = \lambda_{12}\sigma_1 + \lambda_{22}\sigma_2 + \frac{-qcos^2\theta + 2sin^2\theta\frac{X^2}{Y^2}}{2P}\varepsilon_p + \Gamma_4$$

$$\gamma_{12} = \frac{\lambda_{66}}{2}\tau_{12} - \frac{2sin\theta cos\theta\frac{X^2}{S^2}}{2P}\varepsilon_p + \Gamma_5 \quad (18)$$

The integration constants $(\Gamma_3, \Gamma_4, \& \Gamma_5)$ are derived from equating the strain equations of elastic and plastic zones at the separation boundary.

$$\Gamma_3 = X_1[(\bar{\lambda}_{11} - \lambda_{11})cos^2\theta + (\bar{\lambda}_{12} - \lambda_{12})sin^2\theta + \bar{\lambda}_{16}sin\theta cos\theta]$$

$$\Gamma_4 = X_1[(\bar{\lambda}_{11} - \lambda_{22})sin^2\theta + (\bar{\lambda}_{12} - \lambda_{12})cos^2\theta - \bar{\lambda}_{16}sin\theta cos\theta]$$

$$\Gamma_5 = X_1[(\bar{\lambda}_{12} - \bar{\lambda}_{11})sin\theta cos\theta + \frac{\bar{\lambda}_{16}}{2}\cos 2\theta + \frac{\lambda_{66}}{2}sin\theta cos\theta] \quad (19)$$

The plastic strain components are given as,

$$\varepsilon_x = \bar{\lambda}_{11}\sigma_x + K_1\varepsilon_p, \quad \varepsilon_y = \bar{\lambda}_{12}\sigma_x + K_2\varepsilon_p, \quad \& \quad \gamma_{xy} = \frac{\bar{\lambda}_{16}}{2}\sigma_x + K_3\varepsilon_p$$

$$\varepsilon_x = \frac{y}{\rho} \quad \& \quad \sigma_x = \frac{\sigma_y}{P} \quad (20)$$

Where ε_p is obtained as a linear function of y

QALAAI ZANISTSCIENTIFIC JOURNAL
A Scientific Quarterly Refereed Journal Issued by Lebanese French University – Erbil, Kurdistan, Iraq
Vol. (10), No (1), Spring 2025
ISSN 2518-6566 (Online) - ISSN 2518-6558 (Print)

$$\varepsilon_p = a + by \qquad a = \frac{-X\bar{\lambda}_{11}}{(K\bar{\lambda}_{11}+K_1P)} \qquad b = \frac{P}{\rho(K\bar{\lambda}_{11}+K_1P)} \tag{21}$$

$$K_1 = \frac{2cos^4\theta+2sin^4\theta\frac{X^2}{Y^2}+(4\frac{X^2}{S^2}-2q)sin^2\theta cos^2\theta}{2P} \quad K_2 = \frac{-q(sin^4\theta+cos^4\theta)+2(2+\frac{X^2}{Y^2}-2\frac{X^2}{S^2})sin^2\theta cos^2\theta}{2P}$$

$$K_3 = \frac{(q+2)cos^3\theta sin\theta-(q+2\frac{X^2}{Y^2})sin^3\theta cos\theta+2(sin^3\theta cos\theta-cos^3\theta sin\theta)\frac{X^2}{S^2}}{2P} \tag{22}$$

The stress component σ_x varies linearly in the elastic region, it can be written as:

$$\sigma_x = \frac{\varepsilon_x}{\bar{\lambda}_{11}} = \frac{y}{\rho\bar{\lambda}_{11}} \tag{23}$$

At the yield point the plastic region expands from the lower and upper surfaces up to $h_1$and h_2

$$\sigma_x = X_1 = \frac{(h_1=h_2=h)}{\rho\bar{\lambda}_{11}} = \frac{h}{\rho\bar{\lambda}_{11}} \qquad \text{or} \qquad \rho = \frac{h}{X_1\bar{\lambda}_{11}} \tag{24}$$

3.2 Deformations Components

The relation between the strain and displacements can be written as

$$\varepsilon_x = \frac{\partial u}{\partial x} = \frac{y}{\rho} \qquad \varepsilon_y = \frac{\partial v}{\partial y} = \bar{\lambda}_{12}\frac{\sigma_y}{P} + K_2\varepsilon_p \tag{25}$$

After putting ε_p the integration results

$$u = \frac{y}{\rho}x + \left(\frac{\bar{\lambda}_{16}K}{P} + 2K_3\right)\frac{by^2}{2} + \left[\frac{\bar{\lambda}_{16}X}{P} + \frac{\bar{\lambda}_{16}K}{P}a + 2K_3a - \gamma_1\right]y + \Gamma_6$$
$$v = \frac{\bar{\lambda}_{12}X}{P}y + \left(\frac{\bar{\lambda}_{12}K}{P} + K_2\right)ay + \left(\frac{\bar{\lambda}_{12}K}{P} + K_2\right)\frac{by^2}{2} - \frac{x^2}{2\rho} + \gamma_1x + \Gamma_7 \tag{26}$$

The integration constants are evaluated using the boundary conditions at the elastic-plastic boundary where stresses are equal in this region.

$$u = \frac{y}{\rho}x + \left(\frac{\bar{\lambda}_{16}K}{P} + 2K_3\right)\left(\frac{by^2}{2} - \frac{bh^2}{2}\right) + \left[\frac{\bar{\lambda}_{16}X}{P} + \frac{\bar{\lambda}_{16}K}{P}a + 2K_3a - \frac{L}{\rho}\right](y-h) + \frac{Lh}{\rho}$$

QALAAI ZANISTSCIENTIFIC JOURNAL
A Scientific Quarterly Refereed Journal Issued by Lebanese French University – Erbil, Kurdistan, Iraq
Vol. (10), No (1), Spring 2025
ISSN 2518-6566 (Online) - ISSN 2518-6558 (Print)

$$v = \left\{\frac{\bar{\lambda}_{12}X}{P} + a\left(\frac{\bar{\lambda}_{12}K}{P} + K_2\right)\right\}(y-h) + \left(\frac{\bar{\lambda}_{12}K}{P} + K_2\right)\left(\frac{by^2}{2} - \frac{bh^2}{2}\right) - \frac{x^2}{2\rho} + \frac{L}{\rho}x + \frac{\bar{\lambda}_{12}Rh^2}{2} - \frac{L^2}{2\rho} \quad (27)$$

3.3 Elastic-Plastic Boundary (h)

The moment of σ_x at any portion to be equal to the bending moment M. The moment of σ_x is derived as

$$M = 2\left[\frac{X_1h^2w}{3} + \int_h^c \left\{\frac{X+K(a+by)}{P}\right\}wydy\right] \quad (28)$$

The integration results a third order algebraic equation as,

$$h^3 + Bh + D = 0 \quad (29)$$

$$B = \frac{\left[\frac{Xc^2}{2P} + \frac{Kac^2}{2P} - \frac{M}{2w}\right]}{\left[\frac{X_1}{3} - \frac{X}{2P} - \frac{Ka}{2P} - \frac{Kd_1}{3P}\right]}, \qquad B = \frac{\left[\frac{Kd_1c^3}{3P}\right]}{\left[\frac{X_1}{3} - \frac{X}{2P} - \frac{Ka}{2P} - \frac{Kd_1}{3P}\right]}, \ \& \qquad d_1 = \left[\frac{X_1P\bar{\lambda}_{11}}{K\bar{\lambda}_{11} + K_1P}\right]$$

The root of the equation is obtained as:

$$h = \sqrt[3]{\frac{-D + \sqrt{D^2 + \frac{4B^3}{27}}}{2}} + \sqrt[3]{\frac{-D - \sqrt{D^2 + \frac{4B^3}{27}}}{2}} \quad (30)$$

4. Finite Element Analysis

4.1 Finite Element Modeling

Solid structural 3D layered element is used to model the composite laminate beam into many elements as shown in Fig. 2. ANSYS software version 19 is used to model composite laminated structure using finite element method. The first step in the finite element analysis is to simulate the static characteristics of the composite structures using ANSYS macro codes. The model geometry properties have described using these macro codes ANSYS.

QALAAI ZANISTSCIENTIFIC JOURNAL
A Scientific Quarterly Refereed Journal Issued by Lebanese French University – Erbil, Kurdistan, Iraq
Vol. (10), No (1), Spring 2025
ISSN 2518-6566 (Online) - ISSN 2518-6558 (Print)

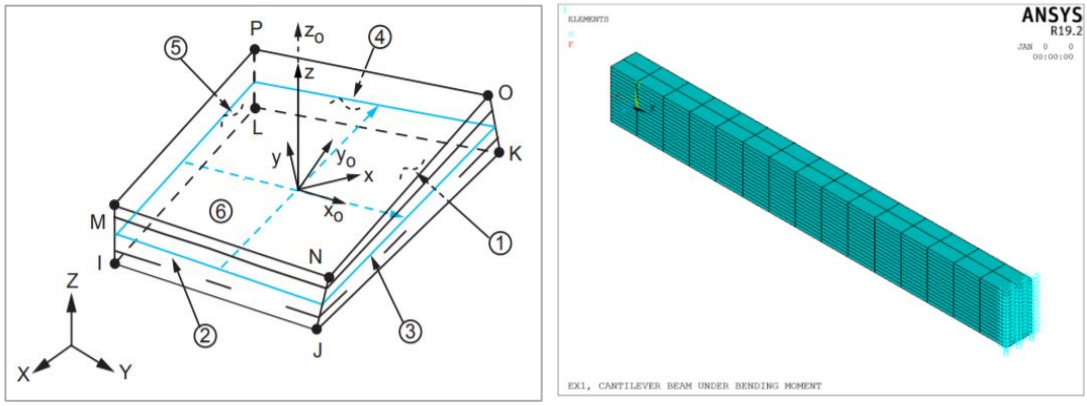

Figure (2): (A)Element type: SOLSH190 layered structural elements (B) Configuration for the finite elements composite beam structure

4.2 Beam dimensions, Material, Element type, and Beam model

Length, width and thickness of the support beam are declared with precision. Also, the material properties reinforced polymer are stated, including Young's modulus Shear modulus, and Poisson's ratio, as shown in Table 1. It is used a composite beam of size (100 mm x 12 mm) and constant thicknesses (7 mm).

Table (1): Material properties of composite laminate beam (All values in Mpa)

E_1	E_2	E_3	G_{12}	G_{13}	G_{23}	υ_{12}	$\bar{X}$	$\bar{S}$	K
13000	13000	13000	400	400	400	0.46	22	11	115

SOLSH190 elements are used as layered structural elements for composite laminated beam as shown in Fig. 2. The defined element type ET of composite material is given in Table 2 as APDL macro codes.

Table (2): Element definition codes

/PREP7 ET,1, SOLSH190 KEYOPT,1,8,1 SECTYPE,1, SHELL	! start the preprocessing ! chooses SOLSH190 element for analysis composite material ! Key option #3 = 1 LAYERED SOLID ELEMENTS

QALAAI ZANISTSCIENTIFIC JOURNAL
A Scientific Quarterly Refereed Journal Issued by Lebanese French University – Erbil, Kurdistan, Iraq
Vol. (10), No (1), Spring 2025
ISSN 2518-6566 (Online) - ISSN 2518-6558 (Print)

Several steps are necessary to create a beam model. Firstly, composite laminated block is created with proper dimensions as given in Table 3 using APDL macro codes. The model structure is divided into many elements as illustrated in Fig. 2. The material characteristics of composite laminate are given in Table 4 as APDL macro codes. Table 5 gives layers thickness, layers numbers, and angles of fiber as APDL macro codes for the composite laminated beam. Clamped boundary condition is applied to edges of fixed ends. NSEL command is used to select nodes in the laminated geometry. D command is used as APDL macro code to assign zero displacement degree of freedom constraints to the laminate edges.

Table (3): Key points generation

/PREP7	! start the preprocessing
K,1,0,0	! corner key points of full (volume)
K,2,L,0	! second corner key points of full (volume)
K,3,L,w	! third corner key points of full (volume)
K,4,0,w	! fourth corner key points of full (volume)
KGEN,2,1,4,1,,,t	! Key points generation in y-axis of full (volume)
L,1,5	! Key points generation in z-axis (volume)
*REPEAT,4,1,1	! connect point 1 with point 2
LESIZE,ALL,,,1	! generating points in length direction
V,1,2,4,3,5,6,8,7	! generating points in width & thickness directions

Table (4): Material Properties codes

/PREP7	! start the preprocessing
MP, EX,1, 13000	! Define Material 1 #: E1=13000 Mpa
MP, EY,1, 13000	! Define Material 1#: E2=13000 Mpa
MP, EZ,1, 13000	! E1=E3=E2 ASSUMED
MP, GXY,1, 400	! Define Material 1#: shear modulus xy-plane G12 =400Mpa
MP, GYZ,1, 400	! Define Material 1#: shear modulus xz-plane G23 =400Mpa
MP, GXZ,1, 400	! Define Material 1#: shear modulus xy-plane G13 =400Mpa
MP, PRXY,1, 0.46	! Define Material 1#: Poisson coefficient υ1 =0.46
MP, PRYZ,1, 0.46	! Define Material 1#: Poisson coefficient υ2 =0.46
MP, PRXZ,1, 0.46	! Define Material 1#: Poisson coefficient υ3 =0.46

QALAAI ZANISTSCIENTIFIC JOURNAL
A Scientific Quarterly Refereed Journal Issued by Lebanese French University – Erbil, Kurdistan, Iraq
Vol. (10), No (1), Spring 2025
ISSN 2518-6566 (Online) - ISSN 2518-6558 (Print)

Table (5): Orientation angles, Thickness, and meshing Composite

/PREP7	! Start the preprocessing
SECTYPE,1, SHELL	! Set #1
L=100	! Total Length
W=12	! Total Width
t=7	! Total Thickness
N=1	! Total Number of Layers
SECDATA, t/N,1,0	! LAYER Thickness, THETA = 0°,15°,30°,45°,60°,75°,90°
ESIZE, ,4	! Initiates the Meshing of all Volume
VMESH,1	! Meshing of all Volume
NSEL,S,LOC,X,0	! Select nodes (x=0)
M1=4664.9	!N.mm
F1=M1/(4*b)	!N
F,1,FX,-F1	! Constrain left end
F,123,FX,-F1	! Select nodes (x=L)
F,22,FX,F1	! Apply load right end
F,143,FX,F1	

5. Results and Discussion

Table 6 lists the elastic, elastic-plastic, residual stress, and corresponding plastic strain components for diverse orientation angles of (0°, 15°, 30°, 45°, 60°, and 90°). As this demonstrates Consequently, the upper and lower surfaces of the beam exhibit the highest intensities of the residual stress component. It is noted that, for the orientation angle of 0, it is the highest residual stress as -8.18 MPa at the lower surface for $h = 3\,mm$. It is also observed from table, any increase in moment couple, it causes a decrease in elastic-plastic boundary h. The maximum equivalent plastic strain occurs at an orientation angle of 45° $(0.061\ for\ h = 3\,mm)$.

A comparison between analytical and finite element is carried out for axial stress component σ_x at the lower surface as given in Table 7. A good agreement is found between analytical and finite element method for several moments M and elastic-plastic boundary h. Table 8 provides the deformations components u and v in the elastic and plastic zones at the free end for orientation angles of (0o, 15o, 30o, 45o, 60o, and 90o).

QALAAI ZANISTSCIENTIFIC JOURNAL
A Scientific Quarterly Refereed Journal Issued by Lebanese French University – Erbil, Kurdistan, Iraq
Vol. (10), No (1), Spring 2025
ISSN 2518-6566 (Online) - ISSN 2518-6558 (Print)

This table demonstrates that the vertical displacement v exceeds the horizontal displacement u. For an orientation angle of 45, v is at its maximum value of $-21.24\ mm$ for $h = 3\ mm$. It is noted that from this table, the vertical displacement component v in the plastic zone is higher at the free end than v in the elastic region.

Contours of residual stress distributions of component σ_x for several orientation angles (0o, 15o, 30o, 45o, 60o, and 90o) versus various elastic-plastic boundary h and diverse moments M as seen in Fig. (3). The borders of plastic part for top and bottom boundaries are observed obviously in this figure. It is also noted that, at the top and bottom roofs, the residual stress component's intensity is at its highest.

Contours of stress distributions of component σ_x for diverse orientation angles versus various elastic-plastic boundary h and diverse moments M as given in Fig. (4). It is clear from figure, the lower edges experience tension stress whereas the upper surface experience compression stress. It is noted that, the values of bending moment M is inversely changes with elastic-plastic boundary h.

The numerical stress results of component σ_x are detected using APDL (Ansys Parametric Design Language) for several orientation angles as drawn as contour distributions in Fig. (5).

QALAAI ZANISTSCIENTIFIC JOURNAL
A Scientific Quarterly Refereed Journal Issued by Lebanese French University – Erbil, Kurdistan, Iraq
Vol. (10), No (1), Spring 2025
ISSN 2518-6566 (Online) - ISSN 2518-6558 (Print)

Table (6): $(x = 0, y = c)$ zone A

$\theta(deg)$	$h(mm)$	$M(N\ mm)$	ε_p	$(\sigma_x)_p(Mpa)$	$(\sigma_x)_e(Mpa)$	$(\sigma_x)_r(Mpa)$
0	3	4664.9	0.0017	22.2	30.37	-8.18
	3.5	4505.3	0.0012	22.14	29.33	-7.19
	4	4324.5	0.0008	22.1	28.15	-6.06
	4.5	4121.8	0.0005	22.06	26.84	-4.77
	5	3896.9	0.0003	22.04	25.37	-3.33
	5.5	3649.4	0.0001	22.02	23.76	-1.74
	6	3379.2	0.0	22.0	22.0	0.0
15	3	4546.3	0.0036	21.75	29.6	-7.85
	3.5	4383.4	0.0025	21.63	28.54	-6.91
	4	4202.7	0.0018	21.54	27.36	-5.817
	4.5	4002.5	0.0012	21.48	26.06	-4.58
	5	3782.1	0.0007	21.43	24.62	-3.2
	5.5	3540.8	0.0003	21.38	23.05	-1.67
	6	3278.3	0.0	21.34	21.34	0.0
30	3	4320.1	0.0056	20.77	28.13	-7.35
	3.5	4158.5	0.0039	20.61	27.07	-6.47
	4	3982.3	0.0027	20.48	25.93	-5.45
	4.5	3789.6	0.0018	20.38	24.67	-4.29
	5	3579.0	0.0011	20.31	23.3	-2.99
	5.5	3349.6	0.0005	20.24	21.81	-1.57
	6	3101.0	0.0	20.19	20.19	0.0
45	3	4216.2	0.0061	20.31	27.45	-7.14
	3.5	4056.6	0.0043	20.13	26.41	-6.28
	4	3883.5	0.0031	19.99	25.28	-5.29
	4.5	3694.7	0.0020	19.89	24.05	-4.17
	5	3488.8	0.0012	19.81	22.71	-2.91
	5.5	3264.9	0.0005	19.74	21.26	-1.52
	6	3022.4	0.0	19.67	19.67	0.0
60	3	4320.1	0.0056	20.77	28.12	-7.35
	3.5	4158.5	0.0039	20.61	27.07	-6.47
	4	3982.3	0.0028	20.48	25.93	-5.45
	4.5	3789.6	0.0018	20.38	24.67	-4.29
	5	3579.0	0.0011	20.31	23.3	-2.99
	5.5	3349.6	0.0005	20.24	21.81	-1.57
	6	3101.0	0.0	20.19	20.19	0.0
90	3	4664.9	0.0016	22.2	30.37	-8.18
	3.5	4505.3	0.0011	22.14	29.33	-7.19
	4	4324.5	0.0008	22.1	28.15	-6.06
	4.5	4121.8	0.0005	22.07	26.84	-4.77
	5	3896.9	0.0003	22.04	25.37	-3.33
	5.5	3649.4	0.0001	22.02	23.76	-1.74
	6	3379.2	0.0	22.0	22.0	0.0

QALAAI ZANISTSCIENTIFIC JOURNAL
A Scientific Quarterly Refereed Journal Issued by Lebanese French University – Erbil, Kurdistan, Iraq
Vol. (10), No (1), Spring 2025
ISSN 2518-6566 (Online) - ISSN 2518-6558 (Print)

Table (7): $(x = 0, y = c)$ zone A

θ	$h(mm)$	$M(N\ mm)$	$(\sigma_x)_{FEM}(Mpa)$	$(\sigma_x)_{ANL}(Mpa)$
0	3	4664.9	31.63	30.37
	3.5	4505.3	30.54	29.33
	4	4324.5	29.32	28.15
	4.5	4121.8	27.94	26.84
	5	3896.9	26.42	25.37
	5.5	3649.4	24.74	23.76
	6	3379.2	22.91	22.0
15	3	4546.3	28.33	29.6
	3.5	4383.4	27.32	28.54
	4	4202.7	26.19	27.36
	4.5	4002.5	24.94	26.06
	5	3782.1	23.57	24.62
	5.5	3540.8	22.07	23.05
	6	3278.3	20.43	21.34
30	3	4320.1	26.30	28.13
	3.5	4158.5	25.39	27.07
	4	3982.3	24.40	25.93
	4.5	3789.6	23.31	24.67
	5	3579.0	21.13	23.3
	5.5	3349.6	19.84	21.81
	6	3101.0	18.44	20.19
45	3	4216.2	25.0	27.45
	3.5	4056.6	24.20	26.41
	4	3883.5	23.33	25.28
	4.5	3694.7	22.38	24.05
	5	3488.8	21.36	22.71
	5.5	3264.9	20.25	21.26
	6	3022.4	17.10	19.67
60	3	4320.1	26.30	28.12
	3.5	4158.5	25.39	27.07
	4	3982.3	24.40	25.93
	4.5	3789.6	23.31	24.67
	5	3579.0	21.13	23.3
	5.5	3349.6	19.84	21.81
	6	3101.0	18.44	20.19
90	3	4664.9	31.63	30.37
	3.5	4505.3	30.54	29.33
	4	4324.5	29.32	28.15
	4.5	4121.8	27.94	26.84
	5	3896.9	26.42	25.37
	5.5	3649.4	24.74	23.76
	6	3379.2	22.91	22.0

QALAAI ZANISTSCIENTIFIC JOURNAL
A Scientific Quarterly Refereed Journal Issued by Lebanese French University – Erbil, Kurdistan, Iraq
Vol. (10), No (1), Spring 2025
ISSN 2518-6566 (Online) - ISSN 2518-6558 (Print)

Table (8): Deformations at A and B zones

			Elastic deformations at zone B $(x=0, y=0)$		Plastic deformations at zone A $(x=0, y=c)$	
$\theta(deg)$	$h(mm)$	$M(N\ mm)$	$u_e\ (mm)$	$\vartheta_e\ (mm)$	$u_p\ (mm)$	$\vartheta_p\ (mm)$
0	3	4664.9	0.0	-1.95	-0.339	-2.825
	3.5	4505.3		-1.88	-0.290	-2.421
	4	4324.5		-1.81	-0.254	-2.119
	4.5	4121.8		-1.72	-0.226	-1.883
	5	3896.9		-1.63	-0.203	-1.695
	5.5	3649.4		-1.52	-0.185	-1.541
	6	3379.2		-1.41	-0.169	-1.413
15	3	4546.3	0.0	-5.41	-0.984	-7.815
	3.5	4383.4		-5.21	-0.846	-6.698
	4	4202.7		-4.99	-0.743	-5.862
	4.5	4002.5		-4.76	-0.662	-5.211
	5	3782.1		-4.49	-0.597	-4.690
	5.5	3540.8		-4.21	-0.544	-4.264
	6	3278.3		-3.89	-0.499	-3.909
30	3	4320.1	0.0	-11.80	-2.082	-16.99
	3.5	4158.5		-11.36	-1.786	-14.57
	4	3982.3		-10.88	-1.565	-12.75
	4.5	3789.6		-10.35	-1.393	-11.33
	5	3579.0		-9.77	-1.254	-10.20
	5.5	3349.6		-9.15	-1.141	-9.27
	6	3101.0		-8.47	-1.05	-8.5
45	3	4216.2	0.0	-14.77	-2.54	-21.24
	3.5	4056.6		-14.21	-2.18	-18.21
	4	3883.5		-13.61	-1.91	-15.93
	4.5	3694.7		-12.95	-1.69	-14.16
	5	3488.8		-12.22	-1.53	-12.75
	5.5	3264.9		-11.44	-1.39	-11.59
	6	3022.4		-10.59	-1.27	-10.63
60	3	4320.1	0.0	-11.80	-1.984	-16.99
	3.5	4158.5		-11.36	-1.699	-14.56
	4	3982.3		-10.88	-1.485	-12.75
	4.5	3789.6		-10.35	-1.319	-11.33
	5	3579.0		-9.77	-1.186	-10.2
	5.5	3349.6		-9.15	-1.077	-9.27
	6	3101.0		-8.47	-0.987	-8.49
90	3	4664.9	0.0	-1.95	-0.339	-2.83
	3.5	4505.3		-1.88	-0.290	-2.42
	4	4324.5		-1.81	-0.254	-2.12
	4.5	4121.8		-1.72	-0.226	-1.88
	5	3896.9		-1.63	-0.203	-1.69
	5.5	3649.4		-1.52	-0.185	-1.54
	6	3379.2		-1.41	-0.169	-1.41

QALAAI ZANISTSCIENTIFIC JOURNAL
A Scientific Quarterly Refereed Journal Issued by Lebanese French University – Erbil, Kurdistan, Iraq
Vol. (10), No (1), Spring 2025
ISSN 2518-6566 (Online) - ISSN 2518-6558 (Print)

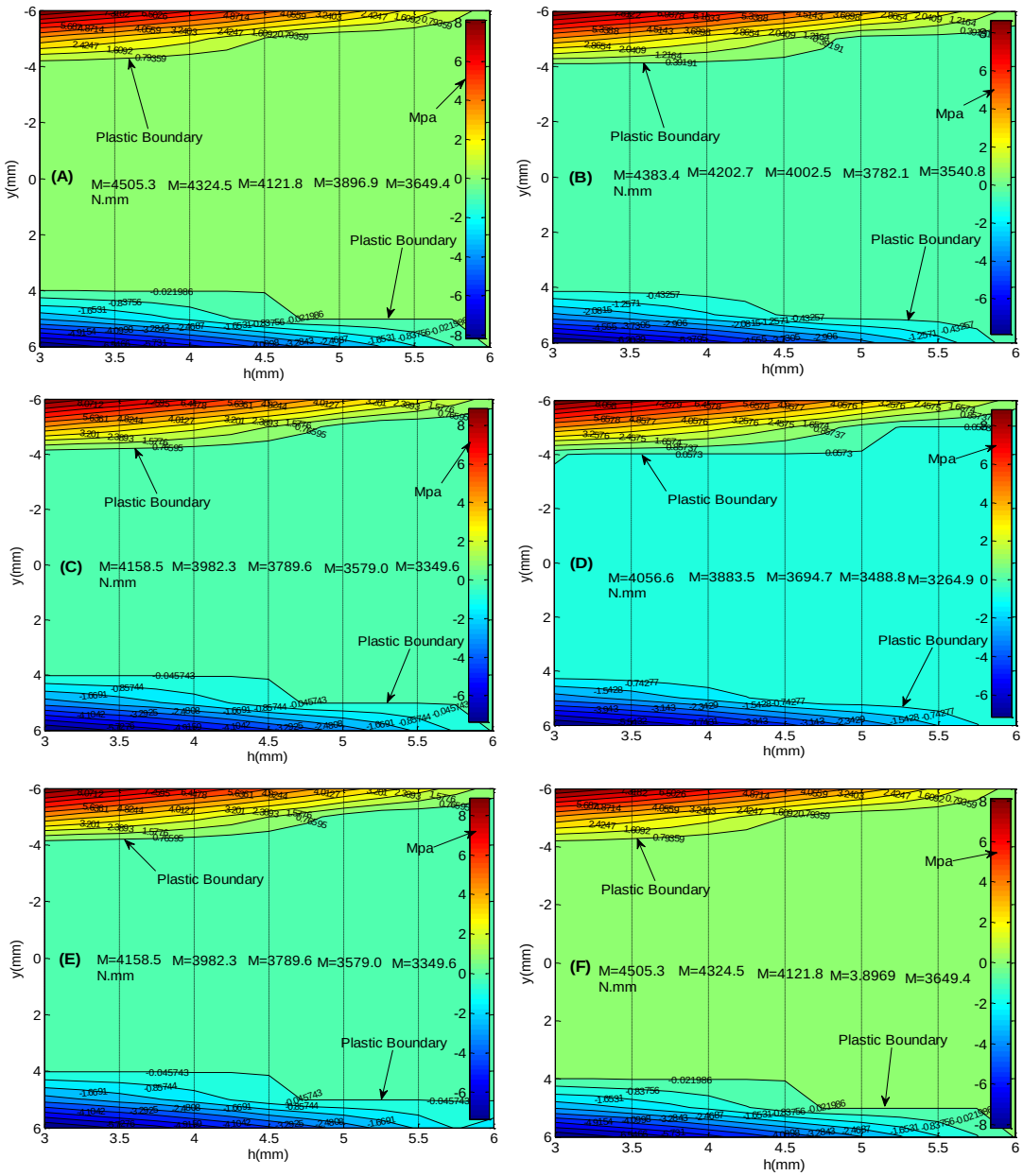

Figure (3): Contours of residual stress distributions of component σ_x for different orientation angles ($(A) = 0^o, (B) = 15^o, (C) = 30^o, (D) = 45^o, (E) = 60^o, (F) = 90^o$)

QALAAI ZANISTSCIENTIFIC JOURNAL
A Scientific Quarterly Refereed Journal Issued by Lebanese French University – Erbil, Kurdistan, Iraq
Vol. (10), No (1), Spring 2025
ISSN 2518-6566 (Online) - ISSN 2518-6558 (Print)

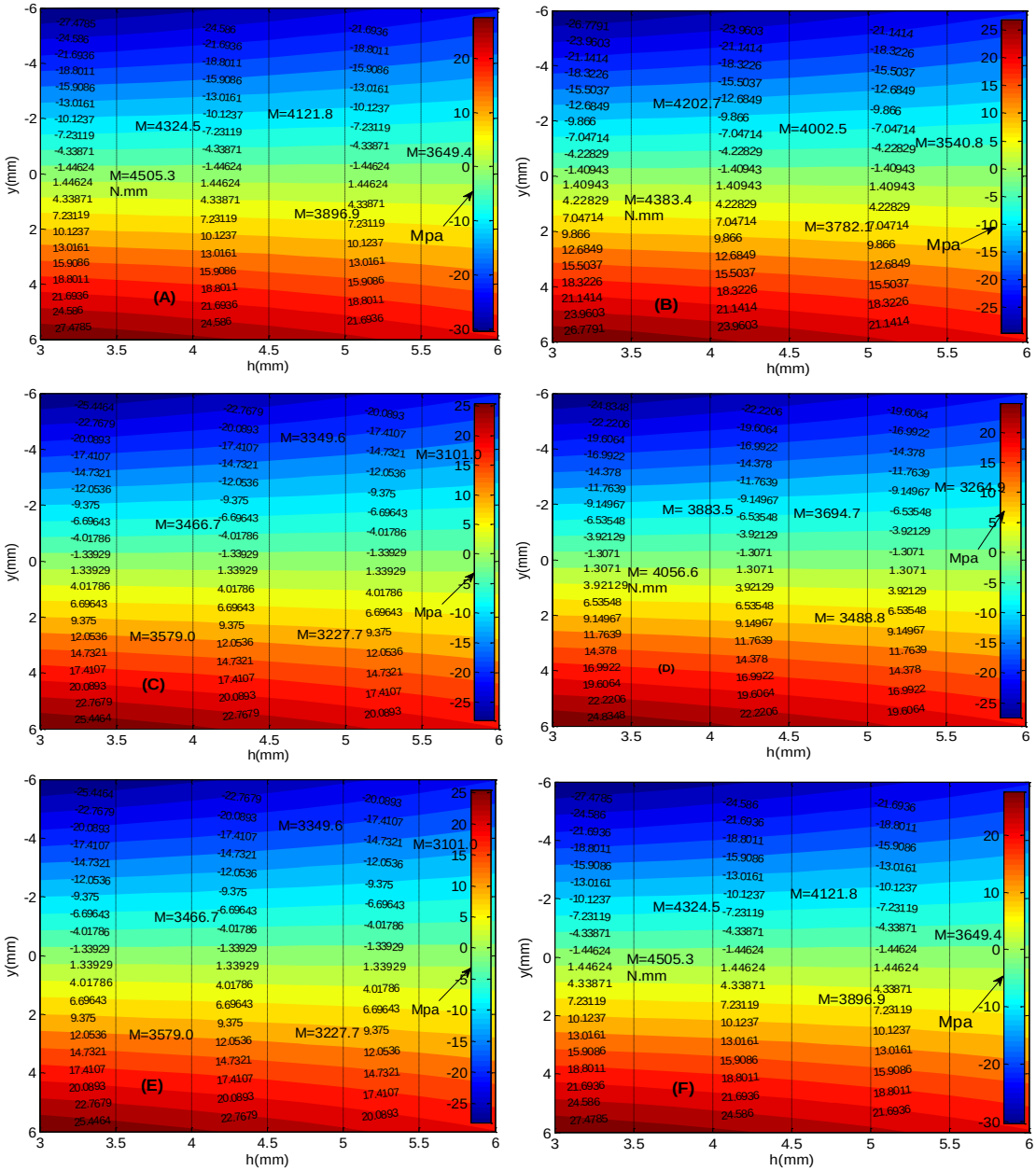

Figure (4): Contours of stress distributions of component σ_x for different orientation angles $((A) = 0^o, (B) = 15^o, (C) = 30^o, (D) = 45^o, (E) = 60^o, (F) = 90^o)$

QALAAI ZANISTSCIENTIFIC JOURNAL
A Scientific Quarterly Refereed Journal Issued by Lebanese French University – Erbil, Kurdistan, Iraq
Vol. (10), No (1), Spring 2025
ISSN 2518-6566 (Online) - ISSN 2518-6558 (Print)

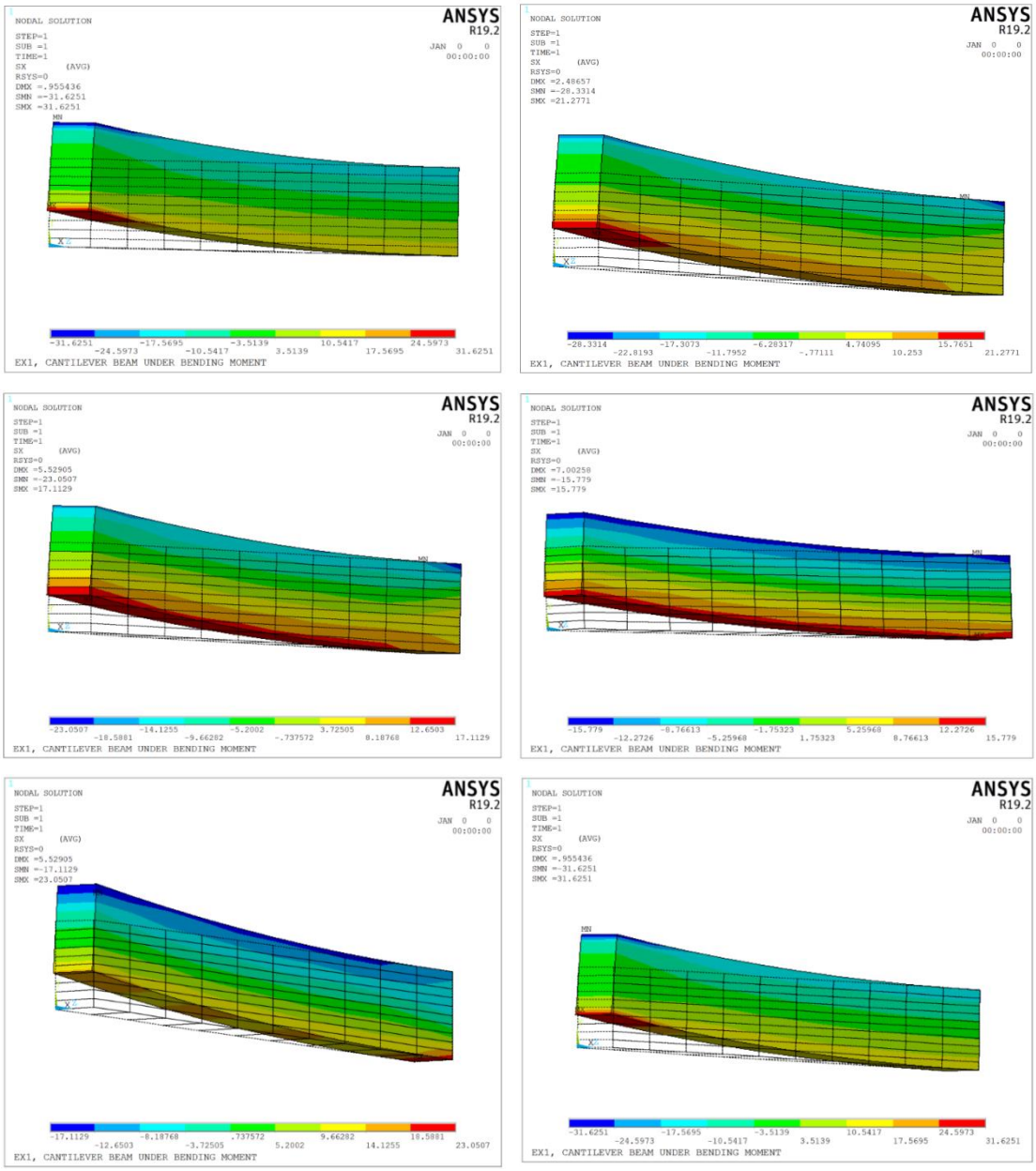

Figure (5): Numerical stresses σ_x(Mpa) for (0º, 15º, 30º, 45º, 60º, and 90º) orientation angles

QALAAI ZANISTSCIENTIFIC JOURNAL
A Scientific Quarterly Refereed Journal Issued by Lebanese French University – Erbil, Kurdistan, Iraq
Vol. (10), No (1), Spring 2025
ISSN 2518-6566 (Online) - ISSN 2518-6558 (Print)

6. Conclusion

The following conclusions are gained from the analytical and finite element solution of the composite beam:

1. The horizontal deformation component of u is lower than the vertical deformation component of v.
2. At the same section, the vertical deformation component in the plastic zone is larger than the vertical deformation in the elastic region.
3. The vertical deformation components at the point $A\ (x = 0, y = c)$ is the greatest for the orientation angle of 45°.
4. For the orientation angle of 0°, the residual stress component of σ_x has the highest concentration.
5. The maximum equivalent plastic strain occurs at an orientation angle of 45°.
6. Highest residual stress occurs at the lower surface for orientation angle of 0°.
7. At the top and bottom roofs of the beam, the residual stress intensity is strongest.

QALAAI ZANISTSCIENTIFIC JOURNAL
A Scientific Quarterly Refereed Journal Issued by Lebanese French University – Erbil, Kurdistan, Iraq
Vol. (10), No (1), Spring 2025
ISSN 2518-6566 (Online) - ISSN 2518-6558 (Print)

References

[1] M.' R., R., B.'H., and L.'J., "Notched Strength of Thermoplastic Woven Fabric Composites," *J Compos Mater*, vol. 29, no. 12, Aug. 1995.
[2] "Frank F. Shi," "The Mechanical Properties and Deformation of Shear-Induced Polymer Liquid Crystalline Fibers in an Engineering Thermoplastic," *J Compos Mater*, vol. 30, no. 14, Oct. 1996.
[3] T. 'I, "Thermal and mechanical properties of aluminum powder-filled high-density polyethylene composites," *Journal of Applied Polymer Science*, vol. 62, no. 12, pp. 2161–2167, Dec. 1996.
[4] "N. Miyazaki" and "T. Hamao," "Solid Particle Erosion of Thermoplastic Resins Reinforced by Short Fibers," *J Compos Mater*, vol. 28, no. 9, May 1994.
[5] "D. R. J. Owen" and "J. A. Figueiras," "Anisotropic elasto-plastic finite element analysis of thick and thin plates and shells," *Int J Numer Methods Eng*, vol. 19, no. 4, pp. 541–566, Apr. 1983.
[6] "G. Jeronimidis" and "A.T. Parkyn," "Residual Stresses in Carbon Fibre-Thermoplastic Matrix Laminates," *Journal of Composite Materials*, vol. 22, no. 5, May 1988.
[7] "Nithin K. Parambil," "Branndon R. Chen," and "Joseph M. Deitzel," "A methodology for predicting processing induced thermal residual stress in thermoplastic composite at the microscale," *Compos B Eng*, vol. 231, Feb. 2022.
[8] "Qi Wu," "Nobuhiro Yoshikawa," and "Nobuhiro Yoshikawa," "Investigation of residual stresses induced by composite forming using macro-micro simulation," *Journal of Reinforced Plastics and Composites*, vol. 39, no. 17–18, Jun. 2020.
[9] "Akay M" and 'OÈ zden S, "The influence of residual stresses on the mechanical and thermal properties of injection moulded ABS copolymer," *J Mater Sci*, pp. 3358–3368, Oct. 2004.
[10]"Ramazan Karakuzu" and "Reşat Özcan," "Exact solution of elasto-plastic stresses in a metal-matrix composite beam of arbitrary orientation subjected to transverse loads," *Compos Sci Technol*, vol. 56, no. 12, pp. 1383–1389, 1996.
[11]"R. Karakuzu," "A. Özel," and "O. Sayman," "Elastic-plastic finite element analysis of metal matrix plates with edge notches," *Comput Struct*, vol. 63, no. 3, pp. 551–558, May 1997.
[12]D. R. J. 'Owen, "Anisotropicelasto-plastic finite element analysis of thick and thin plates and shells," *International Journal for Numerical Methods in Engineering* , vol. 19, no. 4, pp. 541–566, Apr. 1983.
[13]"O. Sayman," "Elasto-plastic stress analysis in stainless steel fiber reinforced aluminum metal matrix laminated plates loaded transversely," *Compos Struct*, vol. 43, no. 2, pp. 147–154, 1998.
[14]"R. Karakuzu" and "O. Sayman," "Elasto-plastic finite element analysis of orthotropic rotating discs with holes," *Comput Struct*, vol. 51, no. 6, pp. 695–703, 1994.

QALAAI ZANISTSCIENTIFIC JOURNAL
A Scientific Quarterly Refereed Journal Issued by Lebanese French University – Erbil, Kurdistan, Iraq
Vol. (10), No (1), Spring 2025
ISSN 2518-6566 (Online) - ISSN 2518-6558 (Print)

[15]B. 'Semih, S. 'Onur, and S. 'Metin, "NUMERICAL ELASTIC PLASTIC STRESS ANALYSIS IN A WOVEN STEEL REINFORCED COMPOSITE THERMOPLASTIC CANTILEVER BEAM ," *Mathematical and Computational Applications*, vol. 17, no. 2, pp. 100–110, 2012.
[16]"Onur SAYMAN," "Ümran ESENDEMİR," and "Ayşe ÖNDÜRÜCÜ," "AN EXACT ELASTO-PLASTIC SOLUTION OF METAL-MATRIX COMPOSITE CANTILEVER BEAM LOADED BY A SINGLE FORCE AT ITS FREE END," *JOURNAL OF ENGINEERING SCIENCES*, vol. 7, no. 3, pp. 313–321, Apr. 2001.
[17]"Mahmood M. Shokrieh," *Residual Stresses in Composite Materials*. Woodhead Publishing Series in Composite Sciences and Engineering, 2014.
[18]"M.R.L. Gower," "R.M. Shaw," "L. Wright," and "J. Urquhart," "Determination of ply level residual stresses in a laminated carbon fibre-reinforced epoxy composite using constant, linear and quadratic variations of the incremental slitting method," *Applied Science and Manufacturing*, vol. 90, pp. 441–450, Nov. 2016.
[19]"Wei Zhang," "Amanda S. Wu," "Jessica Sun," and "Zhenzhen Quan," "Characterization of residual stress and deformation in additively manufactured ABS polymer and composite specimens," *Compos Sci Technol*, vol. 150, no. 29, pp. 102–110, Oct. 2017.
[20]"Hossein Ghayoor Karimiani," "Analysis of Residual Stresses in Thermoplastic Composites Manufactured by Automated Fiber Placement," Master of Applied Sciences (Mechanical Engineering) , CONCORDIA UNIVERSITY, Montreal, Quebec, Canada, 2015.
[21]"J.A. Barnes" and "G.E. Byerly," "The formation of residual stresses in laminated thermoplastic composites," *Compos Sci Technol*, vol. 51, no. 4, pp. 479–494, 1994.
[22]"Sandeep Chava" and "Sirish Namilae," "Continuous evolution of processing induced residual stresses in composites: An in-situ approach," *Applied Science and Manufacturing*, vol. 145, Jun. 2021.
[23]"Beomkeun Kim" and "Juwon Min," "Residual stress distributions and their influence on post-manufacturing deformation of injection-molded plastic parts," *J Mater Process Technol*, vol. 245, pp. 215–226, Jul. 2017.
[24]"Ben Seers" and "Rachel Tomlinson," "Residual stress in fiber reinforced thermosetting composites: A review of measurement techniques," *Polym Compos*, vol. 42, no. 4, pp. 1631–1647, Apr. 2021.

QALAAI ZANISTSCIENTIFIC JOURNAL
A Scientific Quarterly Refereed Journal Issued by Lebanese French University – Erbil, Kurdistan, Iraq
Vol. (10), No (1), Spring 2025
ISSN 2518-6566 (Online) - ISSN 2518-6558 (Print)

شیکردنه وەی فشاری پاشماوەیی بۆ ئاوێتەی ماددەی ئاوێتەی گەرمی لەگەڵ ساتی چەمانەوەی بێهاوتا شیکاری و شیکردنەوەی توخمی کۆتایی

پـوخـتـه:

ڕێگای شیکردنەوەی شیکاری بۆ گریمانەی بڕنۆلی-نافیار گریمان لەگەڵ ڕێگای FEM جۆری APDL بۆ دیاریکردنی فشاری پاشماوەیی لە نێو بیمی ئاوێتە لە ژێر چەمانەوەی تاك بۆ چەند سنوریکی پلاستیکی لاستیکی . ڕیشاڵی پۆلایی تێکەڵکراو لەگەل گۆشەی ئاراستەی جۆراوجۆر (0º,15º and 90º ,30º,45º,60º لەم شیکردنەوەیەدا گریمانە کراوە. هاوکێشەی جیاوازی فەرمانڕەوا و مەرجی سنوور هەردووکیان بە شیکەرەوە چارەسەرکران بۆ حالەتی فشاری ئاست و شێوە گۆڕینی پلاستیکی بچوك. پێوەرەکە لەسەر بنەمای (Tasi-Hill) تیۆری دانراوە. تێبینی ئەوە دەکرێت کە چری پاشماوەکە بەهێزترە لە سەربانەکانی سەرەوە و خوارەوەی بیمەکە. ڕێکەوتنێکی باش دۆزراوە لە نێوان شیکەرەوەی و میتۆدی توخمی کۆتایی بۆ چەند ساتیکی چەمانەوەو سنوری پلاستیکی لاستیکی.

تحليل الأجهاد المتبقي لمواد الألياف المنسوجه والمركبه تحت تأثير عزم الانحناء : دراسه تحليليه وتقربيه بأستخدام (FEM)

الملخص:

تم أستخدام طريقه تحليله بأفتراض فرضيات Bernoulli-Navier والطريقه التقربيه FEM من نوع (APDL) للكشف عن الأجهادات المتبقيه خلال ألياف المواد المنسوجه تحت تأثير عزم الانحناء ولمجموعه قيم مختلفه من الحدود البلاستيكيه المرنه. لقد تم فرض نسج الألياف بزوايا مختلفه (0º, 15º, 30º, 45º, 60º, and 90º) للمواد المركبه. كذلك تم تحليل المعادله التفاضليه وشروط او ظروف الحدود بشكل تحليلي لحاله plane stress بفرض استطالات صغيره. و تم أستخدام نظريه Tsai-Hill في أكتشاف المناطق التي تعاني أعلى أجهادات في الحدود العلويه والسفليه للعتبه المستخدمه. أخيرا تم عمل مقارنه جيده بين الدراسه التحليليه والتقربيه FEM لعده عزوم M ولعده حدود بلاستيكيه مرنه h .